Catalysis Science & Technology

Accepted Manuscript

ROYAL SOCIETY OF CHEMISTRY

www.rsc.org/catalysis

RSCPublishing

ARTICLE

Modeling of enzymatic production of Isomaltooligosaccharides: A mechanistic approach

Cite this: DOI: 10.1039/x0xx00000x

Received ooth January 2012,
Accepted ooth January 2012

DOI: 10.1039/x0xx00000x

www.rsc.org/

A Basu,[a,b] S Mutturi,[c] and S G Prapulla[d]

Enzymatic process of isomaltooligosaccharides (IMO) production from maltose was investigated using in-house produced α-glucosidase from *Aspergillus niger* PFS o8. A reaction mechanism involving fourteen separate enzymatic steps was formulated towards the production of series of higher sugars (DP≥3) contributing to net IMO. The kinetics involving Michaelis–Menten behavior with substrate and product inhibition effects was designed for the formulated reaction mechanism and later the involved kinetic parameters were estimated using a binary genetic algorithm. The influence of various parameters on model behavior is determined by sensitivity analysis. The results suggested that the maximum reaction velocity (v_m) related to maltose to glucose, panose to maltose, isomaltose to glucose, glucosyl-panose to panose and isomaltotriose to isomaltose were sensitive among hydrolysis reactions, whereas among transglucosylation reactions the v_m involved in transglucosylation of maltose to maltotriose and panose, isomaltose to isomaltotriose, maltotriose to maltotetraose, panose to glucosyl-panose and glucose to isomaltose were observed to be critical on the model outcome. Amongst the inhibition parameters the competitive product inhibition of glucose and maltose in the hydrolysis reaction of panose to maltose and competitive product inhibition of glucose on isomaltose hydrolysis were found to be sensitive. To substantiate the formulated model, a validation experiment was carried out at 300 g/l of initial maltose concentration and the experimental results were in good agreement with the model predictions.

1. Introduction

Prebiotics are food ingredients that remain unaffected to digestion and selectively fuel the proliferation and /or activity of desired populations of bacteria native to the human or animal colon *in situ*.[1] Increased demand for sugar and fat free products due to obesity concern and a positive change in the attitude on dairy consumption are likely to boost the demand for prebiotics around the world. The Grand View Research Institute assessed the global prebiotics market and predicted it to reach USD 5.75 billion by 2020, representing nearly 1,084.7 kilo tons, growing at a CAGR of 9.3% from 2014 to 2020.[2] Among these prebiotics, isomaltooligosacchaides (IMO) has received greater attention worldwide for years owing to some of their key properties like mild taste, high temperature and pH stability, low viscosity and low water activity.[3-5]

By definition, IMO are glucosyl saccharides with only α-(1-6) linkages; but commercial accepted IMO syrup is a mixture of glucosyl saccharides with both α-(1-6) and α-(1-4) linkages[6](Fig 1 (a),(b)).The well-known IMOs are isomaltose, panose, isomaltotriose, isomaltotetraose, isopanose and higher branched oligosaccharides. Commercial grade IMO is composed of panose (33%), glucose (25%), isomaltose (20%) and maltose (15%).[7] Although traditionally glucosyl-transferase (EC 2.4.1.24) is used for the conversion of maltose to IMO, α-glucosidase (EC 3.2.1.20), a well-known hydrolyzing enzyme, can also be used to carry out transglucosylation of maltose. The primary role of α-glucosidase is to hydrolyze α-glycosidic linkages from the non-reducing end of oligosaccharides and polysaccharides with the release of α-D-glucose. However, the enzyme also exhibits transferase activity (transglycosylation reaction) at higher substrate concentration, which results in the formation of IMO.[8] The action of α-glucosidase on maltose is shown in Fig 1(c). In the first step of the reaction, a glucose-enzyme intermediate (G-E) is formed which under diluted condition (presence of excess water), is hydrolyzed to glucose. When excess of maltose is present in the reaction medium,

RSCPublishing

ARTICLE

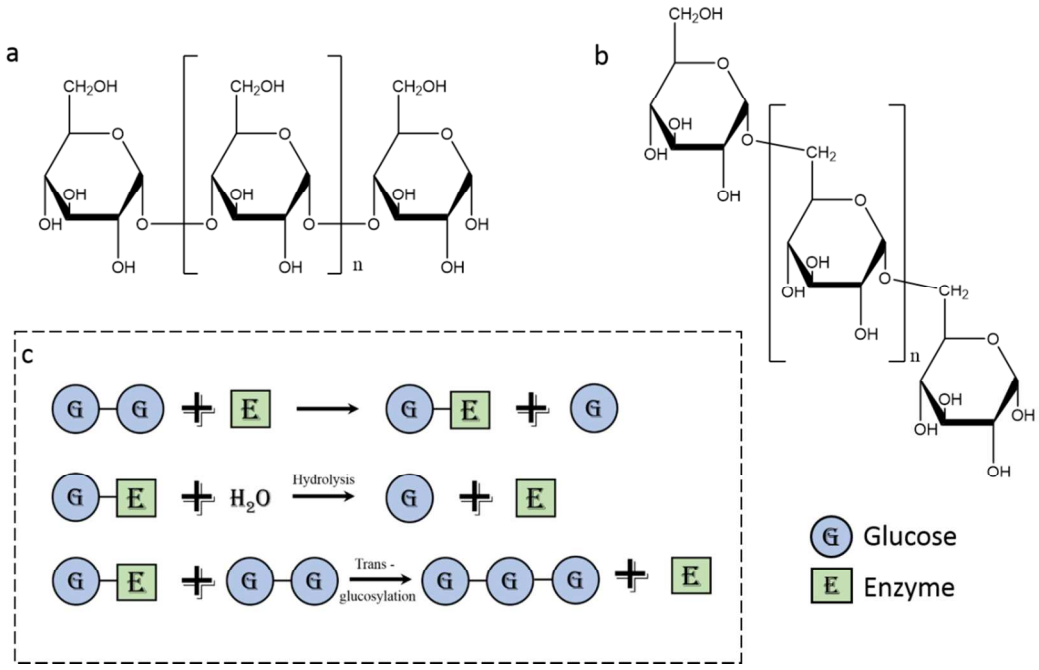

Fig 1 (a) Condensed form of α-(1-4) linked IMO (1≤ n≤ 8) (b) Condensed form of α-(1-6) linked IMO (0≤ n≤ 8) (c) The action of α-glucosidase on maltose.

the glucose moiety from the glucose enzyme intermediate is transferred to the unreacted maltose resulting in trisaccharides. The transfer may occur to any of the OH-group of the acceptor maltose leading to the formation of a series of trisaccharides. When tri-saccharides act as acceptor for the glucosyl residue a series of tetra-saccharides are formed.[9]

The hydrolysis and the transglucosylation reaction of maltose occur concurrently making the mechanism extremely complex. Effective mathematical models for IMO synthesis are of pronounced significance since they would permit easy optimization, scale up of IMO production and would also allow design of a reactor suitable for the purpose. However published reports on mechanistic models that describe IMO production comprehensively are minimal to negligible. Duan *et al.*[10] have investigated the reaction mechanism for IMO production and developed a model for the same[9], however, the authors included only the transglucosylation mechanism at higher maltose concentration and have not considered the hydrolysis in their model construct. For example their study showed a drop in panose concentration after a stipulated reaction time without concomitant increase in any other transglucosylation product. This indicates there was hydrolysis of panose in those experiments and this was not reflected in the modeling studies. The model also overlooked the probable inhibition that could be caused by the liberated glucose on the enzyme. Thus in the present study the authors made a different choice by incorporating all possible hydrolysis kinetics and inhibitions in the model.

Estimation of the parameters involved in a formulated mathematical model is a critical step towards model prediction and several algorithms and tools are developed to perform this task. Genetic Algorithm (GA) - based parameter estimation has gained prominence among direct search techniques as it is based on natural selection and does not require initial values to run the algorithm.[11] Therefore it is amenable for complex enzyme-kinetic reactions involving several parameters whose ranges are difficult to find

RSCPublishing

ARTICLE

experimentally. GA is an adaptive heuristic search algorithm that is built on survival of the fittest of the given population over consecutive generations. Each generation comprises of a population of character strings that are equivalent to the chromosome in DNA while each individual denotes a point in a search space and a possible solution. The individuals in the population are then treated to a process of evolution. It works with a population of points instead of a single point leading to a global solution, hence offering a substantial advantage while searching a large state-space, multi-modal state-space, or n-dimensional surface.[11] GA has been extensively used for estimation of kinetic parameters in models involving chemical and biological processes.[12-15]

The aim of the present study was to develop a comprehensive mechanistic model that would closely describe the kinetics of IMO synthesis from maltose using α-glucosidase. In order to achieve the above task, kinetic experiments were executed to generate experimental data and later a mathematical model was constructed in an attempt to describe the underlying reactions. The model parameters involved were estimated using GA and sensitivity analysis of parameters was carried out to understand the criticality of certain parameters that regulate the formulated reaction mechanism. Finally a validation experiment was carried out to prove the robustness of the developed model.

2. Materials and methods

2.1 Chemicals and microorganism

All the chemicals were of analytical grade. D-maltose, maltotriose, isomaltotriose, isomaltotertrose, panose, isomaltose were procured from Sigma Aldrich (USA). Acetonitrile (HPLC grade) was from Ranbaxy Fine Chemicals Ltd (New Delhi, India). *Aspergillus niger PFS08* was isolated from local paddy field. Isolation and identification of the isolate has been described elsewhere.[16]

2.2 Medium for enzyme production

Aspergillus niger PFS08 was grown in an inoculation medium containing maltose (10 g/l) and yeast extract (2 g/l) (pH 5.5) for 24 h at 29±2 ºC and later 10 % v/v inoculum was transferred into a fermentation medium containing maltose (20 g/l), yeast extract (5 g/l), $NaNO_3$ (10 g/l), $MgSO_4$ $7H_2O$ (0.5 g/l), K_2HPO_4 (2.5 g/l), KH_2PO_4 (2.5 g/l), NH_4Cl (5 g/l), and NaCl (2.5 g/l) , with pH of 5.5. The fermentation was carried out for 192 h at 29±2 ºC. Following cultivation, the broth was centrifuged (4 °C, 5000g) under refrigerated conditions (Remi Industries Pvt. Ltd., Mumbai, India) and the supernatant was used as the source of α-glucosidase without further purification.

2.3 α-glucosidase Assay

The method described by Kato *et al*.[17] was followed to measure α-glucosidase activity using maltose as a substrate. The enzyme was incubated at 40°C with 1% (w/w) maltose solution in 0.5 mM sodium acetate buffer (pH 4) for 15 min. The reaction was arrested by keeping the reaction mixture (RM) in boiling water for 10 min and liberated glucose was measured using a GOD –POD kit (Span Diagonistic Ltd, India). The enzyme assay was performed against two different blank solutions, viz., (a) enzyme blank containing enzyme in acetate buffer and (b) substrate blank containing maltose in acetate buffer and these blanks served to remove background noise of glucose released during cultivation and glucose present as impurity in external maltose added during the assay, respectively. One unit of enzyme activity is defined as the amount of the enzyme that produces 1 µmole of glucose per minute under these conditions.

2.4 Substrate inhibition study

High concentration of maltose (100 g/100 ml) was dissolved in buffer by applying mild heat (60 ºC) and was used as a stock solution. Transglucosylation kinetics by α-glucosidase was studied by varying maltose concentration (50, 100, 200, 300, 400, 500, 600 g/l). Four ml of enzyme (1.6 U/ml) was incubated with 6 ml of maltose (100 % w/v) in citrate buffer (0.05 M, pH 4) at 65 ºC for 1 h. The reaction was terminated by keeping the reaction mixture in boiling water for 15 minutes and the glucose liberated was measured.

RSCPublishing

ARTICLE

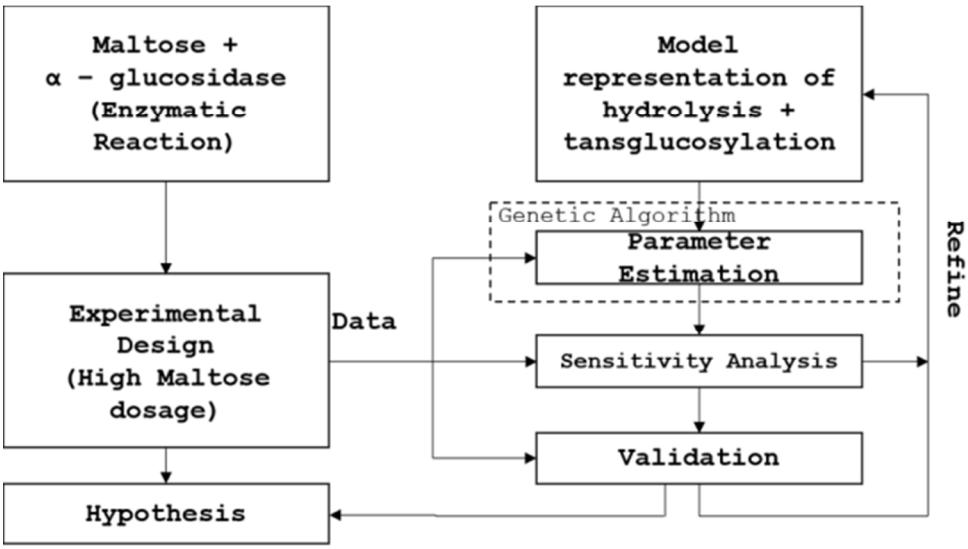

Fig 2 Schematic representation of the methodology used in the study.

2.5 Production of IMO

The cell-free culture fluid after centrifugation was used as the source of α-glucosidase for the production of IMO. The reaction mixture consisted of 6 ml of maltose (100 % w/v) in citrate buffer (0.05M, pH 4) and 4 ml of the enzyme (1.6 U/ml) and the mixture was incubated at 65 ºC for 120 h. Samples were withdrawn at regular intervals, the reaction was arrested by keeping the reaction mixture in boiling water for 15 min. The samples were stored at -20ºC until further use. All experiments were conducted in triplicates.

2.6 Model development

IMO produced from maltose involves a complex combination of simultaneous hydrolysis and transglucosylation reactions. The overall process of model development is summarized in Fig 2. Based on experimental data, it is proposed that formation of isomaltooligosacchaides from maltose involves following reactions:

Hydrolysis Reactions

$$G_2^a \xrightarrow{r_1} 2G \qquad \text{Eq. (1)}$$

$$G_3^a \xrightarrow{r_2} G_2^b + G \qquad \text{Eq. (2)}$$

$$G_3^a \xrightarrow{r_3} G_2^a + G \qquad \text{Eq. (3)}$$

$$G_2^b \xrightarrow{r_4} 2G \qquad \text{Eq. (4)}$$

$$G_3^b \xrightarrow{r_5} G_2^a + G \qquad \text{Eq. (5)}$$

$$G_4^a \xrightarrow{r_6} G_3^b + G \qquad \text{Eq. (6)}$$

$$G_4^b \xrightarrow{r_7} G_3^a + G \qquad \text{Eq. (7)}$$

$$G_3^c \xrightarrow{r_8} G_2^b + G \qquad \text{Eq. (8)}$$

Transglucosylation reactions

$$2G_2^a \xrightarrow{r_9} G_3^b + G \quad \text{Eq. (9)}$$

$$2G_2^a \xrightarrow{r_{10}} G_3^a + G \quad \text{Eq. (10)}$$

$$2G_2^b \xrightarrow{r_{11}} G_3^c + G \quad \text{Eq. (11)}$$

$$2G_3^b \xrightarrow{r_{12}} G_4^a + G \quad \text{Eq. (12)}$$

$$2G_3^a \xrightarrow{r_{13}} G_4^b + G_2^a \quad \text{Eq. (13)}$$

$$2G \xrightarrow{r_{14}} G_2^b \quad \text{Eq. (14)}$$

According to the above described reaction mechanism, the dynamic equations for individual state components are also classified into hydrolysis dynamics and transglucosylation dynamics, and are depicted below:

Hydrolysis

$$\frac{dG}{dt} = \left(\frac{2\times180}{342}\right)(r_1 + r_4) + \left(\frac{180}{504}\right)(r_2 + r_3 + r_5 + r_8) + \left(\frac{180}{666}\right)(r_6 + r_7) \quad \text{Eq. (15)}$$

$$\frac{dG_2^a}{dt} = -r_1 + \left(\frac{342}{504}\right)(r_3 + r_5) \quad \text{Eq. (16)}$$

$$\frac{dG_2^b}{dt} = \left(\frac{342}{504}\right)(r_2 + r_8) - r_4 \quad \text{Eq. (17)}$$

$$\frac{dG_3^a}{dt} = -(r_2 + r_3) + \left(\frac{504}{666}\right)r_7 \quad \text{Eq. (18)}$$

$$\frac{dG_3^b}{dt} = -r_5 + \left(\frac{504}{666}\right)r_6 \quad \text{Eq. (19)}$$

$$\frac{dG_3^c}{dt} = -r_8 \quad \text{Eq. (20)}$$

$$\frac{dG_4^a}{dt} = -r_6 \quad \text{Eq. (21)}$$

$$\frac{dG_4^b}{dt} = -r_7 \quad \text{Eq. (22)}$$

Transglucosylation:

$$\frac{dG}{dt} = \left(\frac{180}{2\times342}\right)(r_9 + r_{10} + r_{11}) - r_{14} \quad \text{Eq. (23)}$$

$$\frac{dG_2^a}{dt} = -(r_9 + r_{10}) + \left(\frac{342}{2\times504}\right)(r_{12} + r_{13}) \quad \text{Eq. (24)}$$

$$\frac{dG_2^b}{dt} = -r_{11} + \left(\frac{342}{2\times180}\right)r_{14} \quad \text{Eq. (25)}$$

$$\frac{dG_3^a}{dt} = \left(\frac{504}{2\times342}\right)r_{10} - r_{13} \quad \text{Eq. (26)}$$

$$\frac{dG_3^b}{dt} = \left(\frac{504}{2\times342}\right)r_9 - r_{12} \quad \text{Eq. (27)}$$

$$\frac{dG_3^c}{dt} = \left(\frac{504}{2\times342}\right)r_{11} \quad \text{Eq. (28)}$$

$$\frac{dG_4^a}{dt} = \left(\frac{666}{2\times504}\right)r_{12} \quad \text{Eq. (29)}$$

$$\frac{dG_4^b}{dt} = \left(\frac{666}{2\times504}\right)r_{13} \quad \text{Eq. (30)}$$

Where G = Glucose, G_2^a = Maltose, G_2^b = Isomaltose, G_3^a = Panose, G_3^b = Maltotriose, G_3^c = Isomaltotriose, G_4^a Maltotetraose and G_4^b = glucosyl-panose. The units for both $\frac{dG_i^l}{dt}$ and r_i is g/(l.h).

The rate of reaction (r) for both hydrolysis (1-8) and transglucosylation (9-14) were assumed to follow steady state Michaelis–Menten (M-M) kinetics. The M-M kinetics involves inhibition kinetics in some reactions and these inhibition terms were adopted either based on the experimental evidence or assumptions as detailed below. The following assumptions were considered during kinetic modeling:

a) Based on separate experimentation it was observed that maltose inhibits its own hydrolysis/transglucosylation at higher concentrations, hence substrate inhibition term is included in Eq. (31) & (39).

b) Panose to isomaltose (Eq. 32), isomaltotriose to isomaltose (Eq. 38) and glucose to isomaltose (Eq. 44) were assumed to follow a simple M-M kinetics without any inhibitions.

c) Maltose to panose (Eq. 40) was assumed to follow M-M kinetics with maltose (substrate) inhibition.

d) Maltotriose to maltotetraose (Eq. 42) and panose to glucosyl-panose (Eq. 43) were assumed to follow maltose (product) inhibition.

e) Isomaltose to glucose (Eq. 34), maltotetraose to maltotriose (Eq. 36), glucosylpanose to panose (Eq. 37) and isomaltose to isomaltotriose (Eq.41) were assumed to follow glucose (product) inhibition. This assumption is also supported by the fact that production of fructooligosaccharides (FOS) and galactooligosaccharide (GOS) were found to be competitively inhibited by glucose.[18-19]

f) Panose to isomaltose (Eq. 32) and maltotriose to maltose (Eq. 35) were assumed to be inhibited by both glucose and maltose (product).

The rate of reaction (r) can be represented as:

$$r_1 = \frac{v_{1r} \times G_2^a}{K_{1M} + \left(1 + \frac{G_2^a}{K_{1iG_2^a}}\right) G_2^a}$$

Eq. (31)

$$r_2 = \frac{v_{2r} \times G_3^a}{K_{2M} + G_3^a}$$

Eq. (32)

$$r_3 = \frac{v_{3r} \times G_3^a}{K_{3M}\left(1 + \frac{G}{K_{3iG}}\right)\left(1 + \frac{G_2^a}{K_{3iG_2^a}}\right) + G_3^a}$$

Eq. (33)

$$r_4 = \frac{v_{4r} \times G_2^a}{K_{4M}\left(1 + \frac{G}{K_{4iG}}\right) + G_2^a}$$

Eq. (34)

$$r_5 = \frac{v_{5r} \times G_3^b}{K_{5M}\left(1 + \frac{G}{K_{5iG}}\right)\left(1 + \frac{G_2^a}{K_{5iG_2^a}}\right) + G_3^b}$$

Eq. (35)

$$r_6 = \frac{v_{6r} \times G_4^a}{K_{6M}\left(1 + \frac{G}{K_{6iG}}\right) + G_4^a}$$

Eq. (36)

$$r_7 = \frac{v_{7r} \times G_4^b}{K_{7M}\left(1 + \frac{G}{K_{7iG}}\right) + G_4^b}$$

Eq. (37)

$$r_8 = \frac{v_{8r} \times G_3^c}{K_{8M} + G_3^c}$$

Eq. (38)

$$r_9 = \frac{v_{9r} \times G_2^a}{K_{9M} + G_2^a\left(1 + \frac{G_2^a}{K_{9iG}}\right)}$$

Eq. (39)

$$r_{10} = \frac{v_{10r} \times G_2^a}{K_{10M} + G_2^a\left(1 + \frac{G_2^a}{K_{10iG}}\right)}$$

Eq. (40)

$$r_{11} = \frac{v_{11r} \times G_2^b}{K_{11M}\left(1 + \frac{G}{K_{11iG}}\right) + G_2^b}$$

Eq. (41)

$$r_{12} = \frac{v_{12r} \times G_3^b}{K_{12M}\left(1+\frac{G_2^a}{K_{12iG_2^a}}\right)+G_3^b}$$

Eq. (42)

$$r_{13} = \frac{v_{13r} \times G_3^a}{K_{13M}\left(1+\frac{G_2^a}{K_{13iG_2^a}}\right)+G_3^a}$$

Eq. (43)

$$r_{14} = \frac{v_{14r} \times G}{K_{14M}+G}$$

Eq. (44)

Where v_{jr} = maximum reaction velocity (g/(l.h))

K_{jM} = Michaelis-Menten constant (g/l)

K_{jiX} = inhibition constant (g/l)

Where *i* stands for inhibition
X stands for the compound involved
j (1,2,3…14) indicates the reactions number

2.7 Parameter estimation

Genetic Algorithm (GA), a search and optimization method, which works by mimicking the evolutionary principles, has been used for parameter estimation.[20] Weighted random pairing was used for selection of parent strings for genetic manipulation. Based on the results obtained in a single generation all the individuals are sorted from higher to lower function values. The top half of the population was retained as a mating pool. Certain probabilities were assigned to each chromosome in this pool such that the one with the maximum concentration has the greatest probability of mating, while the chromosome with the minimum concentration has the lowest probability of mating. A simple single point crossover was used for mating between randomly selected chromosomes based on above weighting method. Thus a new set of individuals (chromosomes) is created to replace the discarded ones. This weighting procedure is also known as roulette wheel weighting.[11,20] To overcome the premature convergence, a single point mutation was used with a probability of 0.05 bit change of a chromosome. The parameter settings for the applied GA–based optimization are summarized in Table 1. A simple binary coded GA was developed by using MATLAB® 2013b on Windows 8.1pro platform with Intel(R) Core(TM) i7-4770 processor and was used for GA optimization. The solution to set of ODEs was obtained using the MATLAB ODE solver, ode15s. This solver uses variable order and variable step-length with implicit numerical differentiation formula (NDF) to compute the solution over each time interval.[21]

Table 1 Parameter settings for the genetic algorithm

	GA configuration
No. of Parameters (N_p)	41
Population size	200
No. of Generations	100
Selection probability	0.5
Mutation probability	0.05
Total bits in a chromosome	200
Objective function[a]	$\sum_{i=1}^{n}\left(\frac{1}{N_p}\sum_{j=1}^{P}\left(\frac{\xi_{\text{sim},ij}-\xi_{\text{exp},ij}}{\xi_{\text{exp},ij}}\right)^2\right)$
Stopping criterion	*either 1E-07 or No. of Generations*

[a] $\xi_{sim,ij}$ represents simulated data, $\xi_{exp,ij}$ represents the experimental data for every point (p) for a given state variable, and N_p is the total no. of data point.

2.8 Parametric sensitivity analysis

Sensitivity of model parameters was determined following the method described by Alvarado-Huallanco and Maugeri-Filho.[22] The sensitivity approves the assessment of deviations in the output of the system and hence has a very precise contribution to the model. The sensitivity of a system denotes a change in output variable that can be ascribed to a variation in one of the input parameters of the system. In order to examine the impact of the process variables on the synthesis of IMO, the sensitivity factor as given by Eq. (45) was used, where V_{out} is the output variable (IMO production after 24 h of reaction), V_{in} is the input variable (kinetic parameters), the subscript 'r' is the standard reference condition and 'c' is the changed condition.

$$SF = \frac{\frac{V_{outc} - V_{outr}}{V_{outr}}}{\frac{V_{inc} - V_{inr}}{V_{inr}}} \quad \text{Eq. (45)}$$

Sensitivity factor can be taken as the percentage alteration in output variable for every 1% variation in the input variables. We investigated all the parameters after bringing a positive change of 25% in the input variables. The model equations were simultaneously integrated using the MATLAB® 2013b on Windows 8.1pro platform with Intel(R) Core(TM) i7-4770 processor.

2.9 HPLC analysis

Quantitative analyses of IMO were performed on a HPLC LC-20A (Shimadzu, Japan) equipped with a refractive index detector(RID 20A) (Shimadzu, Kyoto, Japan). Oligosaccharides were separated using amino propyl column (250 mm × 4.6 mm SS Excil amino 5 µm (Santa Clara, California) with isocratic elution using acetonitrile/water (65:35) at a flow rate of 1.0 ml/ min. Samples were suitably diluted and filtered through cellulose nitrate membrane (0.45 µm) before injection (20 µl). All the products in the reaction mixture (RM) were identified by comparing the retention times with those of standards. Product quantification was based on the comparison of peak areas with those of standard sugars. The net IMO at a given time was calculated as a summation of isomaltose, maltotriose, panose, isomaltotriose, maltotetraose and glucosyl-panose concentrations at that time during the reaction. The yield and productivity of IMO at any reaction time was calculated using the following equations:

$$Yield(g\ of\ IMO / g\ of\ maltose) = \frac{IMO_{Final} - IMO_{Initial}}{Maltose_{Initial} - Maltose_{Final}} \quad \text{Eq. (46)}$$

3. Results and discussion

3.1 Maltose inhibition

The kinetic experiment was carried at different initial maltose concentrations ranging from 50 to 600 g/l to examine the (inhibition) effect of maltose concentration on products formed. Initial rate of the reaction were observed by measuring the glucose concentrations at various time intervals during the batch studies as described in earlier section. The results of kinetic experiment (Fig 3) showed that the reaction velocity (v) rose to a maximum (or 1/v reached minimum) and then descended (or 1/v increased) as the maltose concentration increased to more than 200 g/l ($1/S \leq 0.005$). The experimental results indicated a typical substrate inhibition kinetics. It was observed that the rate increased (1/v decreased) linearly with increasing substrate concentration up to 100 g/l ($1/S \geq 0.01$) for the selected intermediate concentrations, beyond this the rate of reaction warded off from the linear phase to lower incremental slope in a non-linear phase between 100 and 200 g/l ($0.01 \leq 1/S \leq 0.005$). Once the selected maltose concentration increased above 200 g/l ($1/S \leq 0.005$) the reaction velocity entered a non-linear deceleration phase indicating strong substrate inhibition of maltose. Here, M-M kinetics involving substrate inhibition was used to fit the experimental results, and the parameters were estimated graphically. Considering there is no substrate inhibition in the concentration range of 50 g/l to 200 g/l the parameter values were v_m = 363.64 g/(l.h) and K_m = 333.33 g/l. Whereas considering substrate inhibition in the range 300 g/l to 600 g/l the parameter values were observed to be $K_{SI} = 2.98 \times 10^{-5}$ g/l and v_m = 0.0074 g/(l.h). The dropping of v_m from 363.64 g/(l.h) to 0.0074 g/(l.h) indicates a strong inhibition of substrate above 200 g/l.

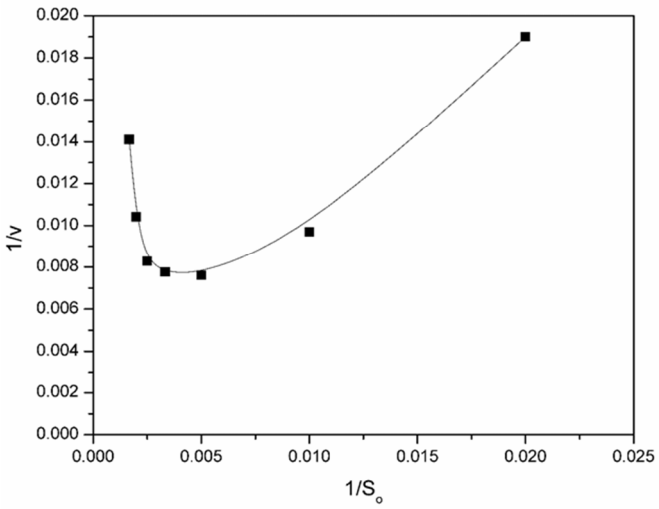

Fig 3 Lineweaver – Burk plot of enzyme reaction rates at different maltose concentration with 1.6 U/ml enzyme, pH 4 and temperature 65°C.

3.2 Production of IMO in batch experiments

An enzyme-substrate experiment was carried out using high dosage of maltose (600 g/l) to generate all possible intermediates and products formed during the reaction setup spanning both hydrolysis and transglucosylation. The production of IMO was found to vary with the time of reaction in a non-linear fashion. A typical time course concentration profile of the products present in the reaction mixture is shown in Fig 4. During the first 20 h of incubation of the reaction, the concentrations of glucose and panose were observed to increase while the latter reached a maximum of 201.4 g/l (Fig 4a and Fig 4d). As shown in Fig 4f, maltotriose was also formed during this period with concentration reaching maximum of 54.42 g/l. Maltotetraose production was initiated at the end of 6 h and reached maximum (20.06 g/l) by 20 h of reaction (Fig 4g). The other tetrasaccharide that was detected in the reaction mixture was glucosyl-panose and its production began at the end of 4 h and thereafter increased gradually reaching a maximum of 39.16 g/l after 36 h of reaction time (Fig 4h). Isomaltose was mainly produced after 6 h of reaction when sufficient amount of glucose was accumulated in the reaction mixture and reached to 70 g/l after 60 h of reaction time (Fig 4c). Production of isomaltotriose (DP_3) was found to be initiated after 12 h and followed saturation kind of kinetics to achieve a maximum concentration of 8.26 g/l at the end of 36 h (Fig 4e). It was observed that the total IMO concentration has reached a maximum value at the end of 24 h of incubation and decelerated beyond this time period. This may be due to the predominance of hydrolysis reactions over transglucosylation reactions. The IMO mixture consisted of panose (189.50 g/l), isomoltose (47.53 g/l), moltotriose (16.28 g/l), isomaltotriose (7.67 g/l) and tetrasaccharides (51.54 g/l). The reaction mixture also contained unreacted maltose (28.69 g/l) and the released glucose (249.85 g/l). The α-glucosidases from *Xantophyllomyces dendrorhous*[8] and *Aspergillus carbonarious*[10] have been reported to produce IMO with similar composition. However IMO composition obtained in the present study is in contrast to other IMO studies where α-glucosidase produced from *A. niger*[9], *A. nidulans*[17] yielded higher isomaltose instead of panose. Similarly in other studies where α-glucosidase was produced from *Acremonium* sp.[23] and *Paecilomyces lilacinus*[24] , the enzymatic reaction yielded oligosaccharides containing only α-(1,2) linkages, and α-(1,2) and α-(1,3) linkages, respectively.

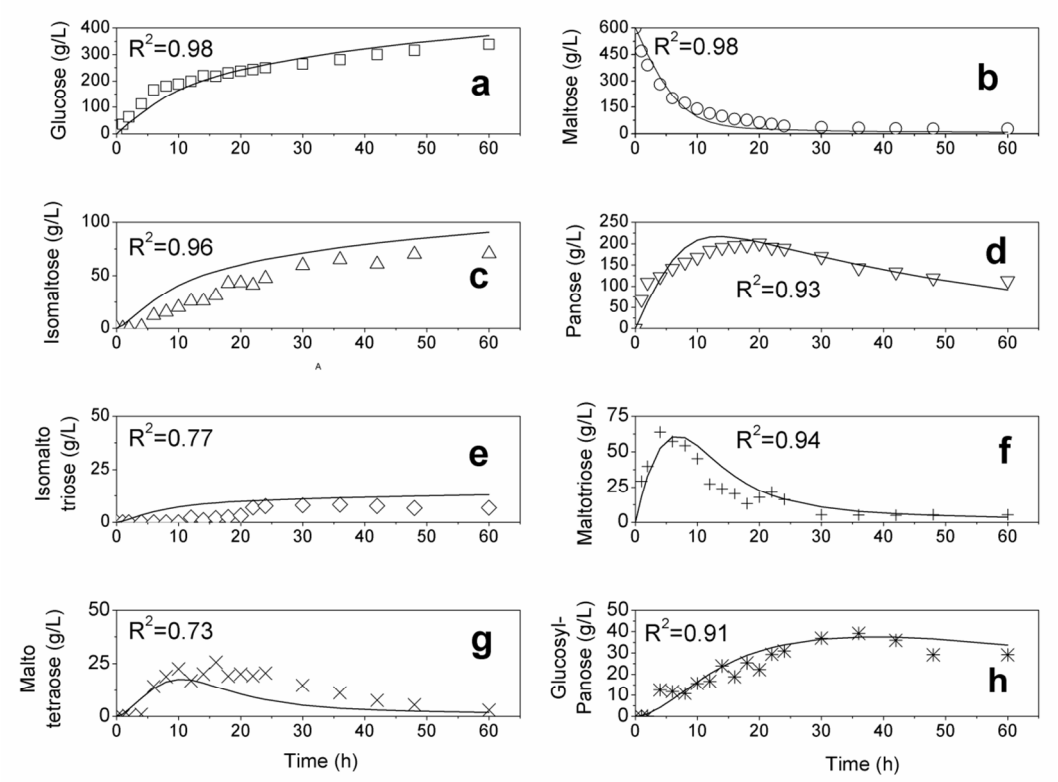

Fig 4 Comparison between experimental values (symbols) and model predicted data (lines) at maltose 600 g/l, enzyme concentration 1.6 U/ml , pH 4 and temperature 65°C

RSCPublishing

ARTICLE

3.3 Model development

The present study was aimed in formulating a comprehensive mechanistic model for enzymatic production of IMO using α-glucosidase. Based on experimental evidence the reaction mechanism was formulated involving all possible hydrolysis (Eq. 1 to 8) and transglucosylation (Eq. 9 to 14) reactions. Among these the transglucosylation reactions were adapted from Duan *et al.*[10] and hydrolysis reactions were based on experimental evidence. It has been observed in the enzyme database, BRENDA, that α-glucosidase was not reported to cleave α-1,6 linkage, however, our study indicated that panose dissociates into maltose and isomaltose in hydrolysis reaction thus indicating the cleavage of α-1,6 linkage (results not shown). Hence both these reactions are included in the hydrolysis set. Moreover, when hydrolysis of panose to isomaltose was ignored in the reaction mechanism the objective function never reached to an optimal solution during parameter estimation, hence this substantiates the experimental evidence of hydrolysis panose to isomaltose.

Earlier studies carried by Duan *et al.*[10] have shown the reaction mechanism for IMO production and was later used to develop a reaction model[9]. However, these studies do not discuss the kinetic equations considered in the modeling. Moreover, hydrolysis reactions were ignored in their proposed reaction mechanism. In the present study efforts were directed towards developing a mechanistic model for IMO production in a comprehensive manner by considering all possible inhibitions (both substrate and product) and reaction outputs. Maltose inhibition and hydrolysis of IMO has been established through experiments. Inclusion of glucose inhibition in the model was assumed based on the logic that concentration of glucose was fairly high in the reaction mixture as shown in Fig 4a. In addition to this, it has also been observed that fructooligosaccharides (FOS) and galactooligosaccharide (GOS) were inhibited by sucrose or lactose respectively and also by liberated glucose.[18-19] The model with inhibitions also resulted in better fits than model without inhibition (results not shown).

3.4 Parameter estimation

The model parameters were estimated at the experimental condition of 600 g/l maltose, 1.6 U/ml of enzyme at 65^{o} C and pH 4. The objective function which is a relative error of experimental and estimated values was minimized by employing the genetic algorithm to the settings mentioned in Table 1. The Table 2 shows the model estimated values of forty one kinetic parameters used for the formulated reaction mechanism. Among the hydrolysis reaction parameters, maximum reaction velocity of isomaltose hydrolysis, v_{8r} (991.46 g/(l.h)) and maximum reaction velocity of isomaltotriose hydrolysis, v_{4r} 982.19 g/(l.h) were observed to be very high, whereas maximum reaction velocity of maltose hydrolysis, v_{1r} (18.12 g/(l.h)), maximum reaction velocity of maltotriose hydrolysis,v_{5r} (8.81 g/(l.h)) and maximum reaction velocity of panose hydrolysis, v_{2r} (0.004 g/(l.h)) were found to have very low values. All transglucosylation reaction parameters were observed to have lower values in comparison to hydrolyis except v_{11r} (maximum reaction velocity of reaction in Eq. 11) which exhibited high value of 907.33 g/(l.h). Among the inhibition parameters, competitive inhibition constant by maltose for panose as substrate, K_{3iG2} (95.28 g/l) and competitive inhibition constant by glucose for maltotriose as substrate, K_{5iG} (27.70 g/l) were found to affect the oligosaccharide production.

The results of parameter estimation suggested that hydrolysis of isomaltose to glucose and isomalotriose to isomaltose are the most significant reactions as evident by the higher v_r values (reaction rates). This finding is quite unusual since both isomaltotriose and isomaltose contain α-1-6 linkage and are supposed to be resistant to α-glucosidase. The results also showed that panose hydrolyzes more to maltose than to isomaltose. This finding is consistent with the experimental data. Rate of hydrolysis of maltose, maltotriose and glucosyl-panose were found to be less compared to others. Among the transglucosylation reaction, rate of formation of isomaltotriose from isomaltose was found to be highest whereas the rate of formation of glucosyl-panose from panose was found lowest. It was also found that transfer of glucose moiety occurred equally to the 4-OH and 6-OH of maltose leading to the formation of maltotriose and panose. Among the inhibition parameters only inhibition of maltose

on panose hydrolysis and inhibition of glucose on maltotriose hydrolysis were found to be substantial.

Table 2 Estimated kinetic parameters for IMO production under the selected kinetic model

Serial No.	Parameter[a]	Value	Units	Serial No.	Parameter[a]	Value	Units
1	v_{1r}	18.12	g/(l.h)	**22**	K_{7iG}	202.50	g/l
2	K_{1M}	86.15	g/l	**23**	v_{8r}	991.46	g/(l.h)
3	K_{1iG2}	640.84	g/l	**24**	K_{8M}	269.39	g/l
4	v_{2r}	0.004	g/(l.h)	**25**	v_{9r}	84.16	g/(l.h)
5	K_{2M}	799.00	g/l	**26**	K_{9M}	763.43	g/l
6	v_{3r}	43.48	g/(l.h)	**27**	K_{9iG2}	851.76	g/l
7	K_{3M}	705.36	g/l	**28**	v_{10r}	127.65	g/(l.h)
8	K_{3iG}	172.32	g/l	**29**	K_{10M}	538.14	g/l
9	K_{3iG2}	95.28	g/l	**30**	K_{10iG2}	601.19	g/l
10	v_{4r}	982.19	g/(l.h)	**31**	v_{11r}	907.33	g/(l.h)
11	K_{4M}	856.31	g/l	**32**	K_{11M}	784.70	g/l
12	K_{4iG}	750.47	g/l	**33**	K_{11iG}	638.30	g/l
13	v_{5r}	8.81	g/(l.h)	**34**	v_{12r}	360.72	g/(l.h)
14	K_{5M}	257.18	g/l	**35**	K_{12M}	822.12	g/l
15	K_{5iG}	27.70	g/l	**36**	K_{12iG2}	667.17	g/l
16	K_{5iG2}	892.28	g/l	**37**	v_{13r}	15.06	g/(l.h)
17	v_{6r}	765.75	g/(l.h)	**38**	K_{13M}	255.89	g/l
18	K_{6M}	791.39	g/l	**39**	K_{13iG2}	872.12	g/l
19	K_{6iG}	538.99	g/l	**40**	v_{14r}	213.93	g/(l.h)
20	v_{7r}	241.54	g/(l.h)	**41**	K_{14M}	411.75	g/(l.h)
21	K_{7M}	983.10	g/l				

[a] v_{jr} = maximum reaction velocity (g/(l.h)), K_{jM} = Michaelis-Menten constant (g/l), K_{jiX} = inhibition constant (g/l) (i stands for inhibition, X stands for the compound involved j (1, 2, 3…14) indicates the reactions number.)

RSCPublishing

ARTICLE

3.5 Parametric sensitivity analysis

The sensitivity of the model to parameter perturbations produces valuable information regarding which parameters variables are most imperative, and the time periods over which they matter most. The sensitivities may be used off-line to analyze controller hitches and may specify the necessity for a better model for the process, additional or altered measurements, or changes in strategy[25]. Therefore, a sensitivity analysis of the model was performed on all of the parameters involved. Fig 5 shows sensitivity of the model parameters under study. A sensitivity value greater than 0.05 has been considered to be substantial and means that a small change in these parameters have significant influence on the model outcome and thus prove the critical nature of the parameter in the reaction mechanism. It can be seen that the most critical parameters were $\mathbf{v_{1r}}$, $\mathbf{v_{3r}}$, $\mathbf{v_{4r}}$, $\mathbf{v_{7r}}$, $\mathbf{v_{8r}}$, $\mathbf{v_{9r}}$, $\mathbf{v_{10r}}$, $\mathbf{v_{11r}}$, $\mathbf{v_{12r}}$, $\mathbf{v_{13r}}$, , $\mathbf{v_{14r}}$, $\mathbf{K_{4M}}$, $\mathbf{K_{10M}}$, $\mathbf{K_{14M}}$, $\mathbf{K_{3iG}}$, $\mathbf{K_{3iG2}}$ and $\mathbf{K_{4iG}}$, which led to higher SF values (Fig 5). Relatively less influential but still relevant parameters were $\mathbf{v_{2r}}$, $\mathbf{v_{5r}}$, $\mathbf{v_{6r}}$, $\mathbf{K_{2M}}$, $\mathbf{K_{3M}}$, $\mathbf{K_{5M}}$, $\mathbf{K_{9M}}$ $\mathbf{K_{1iG2}}$, $\mathbf{K_{5iG}}$, $\mathbf{K_{5iG2}}$, $\mathbf{K_{6iG}}$, $\mathbf{K_{7iG}}$, $\mathbf{K_{9iG2}}$, $\mathbf{K_{10iG2}}$, $\mathbf{K_{11iG}}$, $\mathbf{K_{12iG2}}$ **and** $\mathbf{K_{13iG2}}$, which has a SF value between 0.02 to 0.05. The remaining parameters were observed to have very low SF values (less than 0.02) and can be considered as irrelevant with respect to the model and can also be eliminated so as to reduce the number of parameters. These parameters include $\mathbf{K_{1M}}$, $\mathbf{K_{6M}}$, $\mathbf{K_{7M}}$, $\mathbf{K_{8M}}$, $\mathbf{K_{11M}}$, $\mathbf{K_{12M}}$, $\mathbf{K_{13M}}$. Simulations were carried out by eliminating above non-sensitive parameters one at a time from the model structure and it was observed that the predictions did not significantly change from the original, indicating the insensitivity of those parameters in the formulated model.

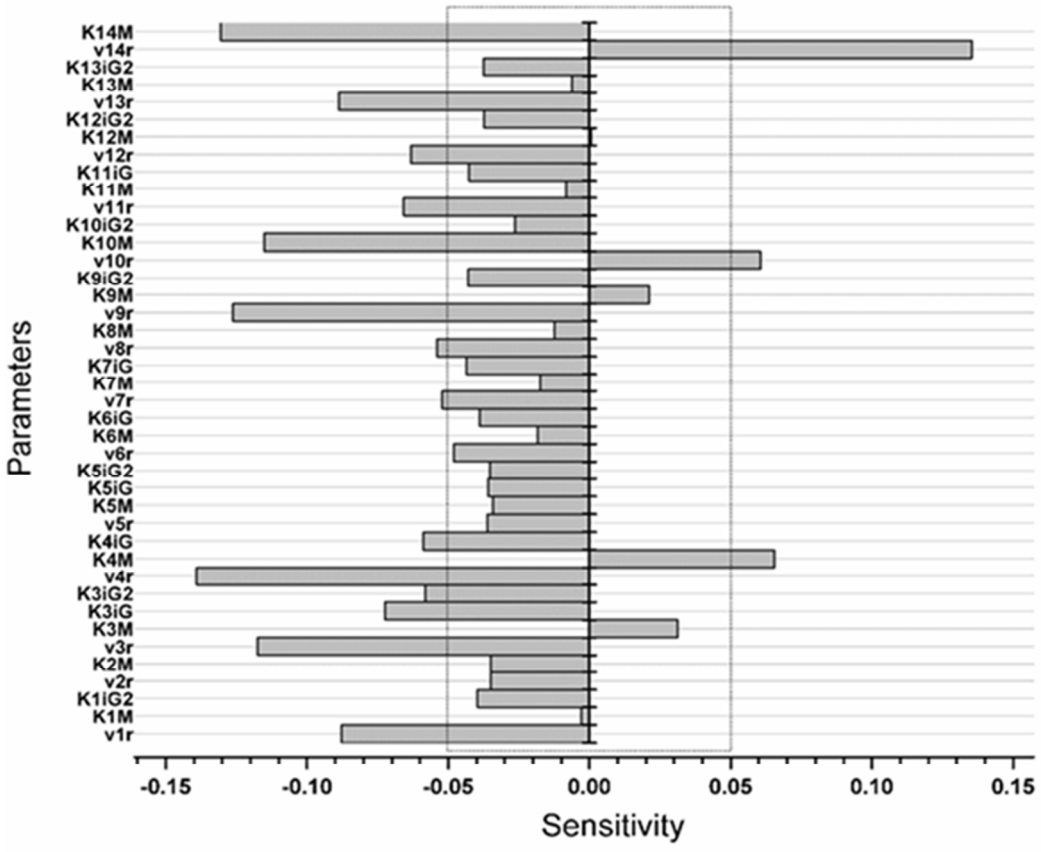

Fig 5 Sensitivity factors (SF) of different kinetic parameters after 24 h of reaction

RSCPublishing

ARTICLE

The results of sensitivity analysis suggested that reaction velocity parameter related to the hydrolysis of maltose to glucose, panose to maltose, isomaltose to glucose, glucosyl-panose to panose and isomaltotriose to isomaltose and transglucosylation of maltose to maltotriose and panose , isomaltose to isomaltotriose, maltotriose to maltotetraose, panose to glucosyl-panose and glucose to isomaltose were extremely substantial whereas hydrolysis of panose to isomaltose, maltotriose to maltose, maltotetrose to maltotriose affected the system moderately. Furthermore it can also be noted that the affinity of the enzyme towards isomaltose for the production of glucose, maltose for the production of panose, and glucose for the production of isomalose were exceedingly critical for the model prediction. All other affinity parameters were found to be either intermediately relevant or unimportant for the model. Amongst the inhibition parameters only the competitive inhibition constant of glucose and maltose on the enzyme for the hydrolysis of panose to maltose and competitive inhibition constant of glucose on isomaltose hydrolysis were found to be appropriate for the model fitting. All other inhibition parameters were observed to be irrelevant for model fitting and could therefore be removed from the model structure. These results are useful for the model reduction and fine tuning of the formulated model.

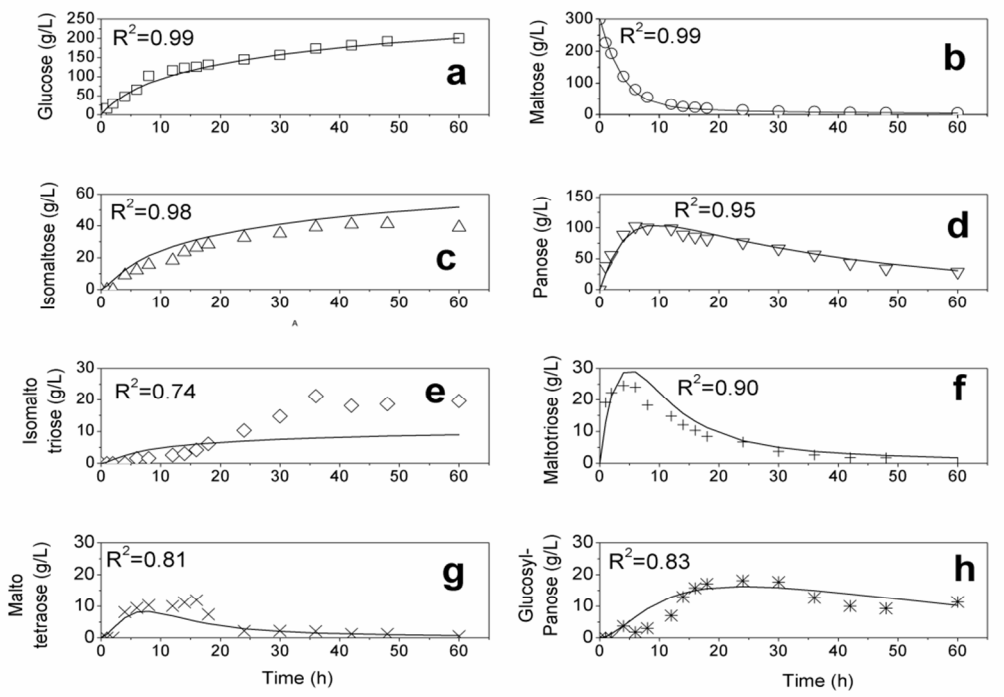

Fig 6 Comparison between experimental values (symbols) and model predicted data (lines) at maltose 300 g/l, enzyme concentration 1.6 U/ml, pH 4 and temperature 65°C.

3.6 Experimental validation of the model prediction

Model validation was carried out at 300 g/l maltose keeping all other reaction conditions same with the parameter values mentioned in Table 2. It was observed that lowering the initial maltose dosage by half i.e from 600 g/l to 300 g/l, resulted in a fairly comparable decrease in nearly all the components in the reaction mixture as evident from the Table 3. It was also observed that hydrolysis of

IMO started after 24 h of reaction when 600 g/l maltose was used; whereas, in case of 300 g/l of maltose the IMO hydrolysis began after 16 h reaction. It can also be noted that the yield of IMO from maltose was 0.56 g of IMO/g of maltose when the initial dosage of maltose was 600g/l after 24 h of reaction and 0.55 g of IMO/g of maltose after 16 h of reaction at an initial maltose concentration of 300g/l (Table 3). The model predicted values were in accordance with that of experimental values (Fig 6) as revealed by the correlation coefficient (R^2) values. The R^2 values for isomaltotriose, maltoteraose and glucosyl-panose were found to be lower than others, however, in this complex reaction mechanism the overall fitness observed was highly reasonable. These results substantiated the robustness of the model in predicting the trend, concentration and yield of IMO production with a change in the input parameter. In addition to that the model also predicted the decreasing trend in IMO formation clearly justifying the inclusion of IMO hydrolysis reactions in the model. This is in contrast to the earlier report by Duan *et al.*[9] which considered only transglucosylation in their model for IMO production. At both the concentrations it was observed that the IMO concentration decreased after a certain time, as hydrolysis of IMO dominated over transglucosylation, resulting in a decline in overall yield and increase in undesirable glucose concentration in the reaction mixture. Fed batch- based reactor setup could be a potential alternative wherein maltose can be fed to the reactor at a time when hydrolysis takes over transglucosylation, in order to improve the yields and productivity of IMO

Table 3 Comparison between IMO produced from 600g/l and 300g/l maltose and their estimated yield

Component (g/l)	Initial Maltose dosage			
	600 g/l[a]		300 g/l[b]	
	Experimental	Predicted	Experimental	Predicted
Glucose	249.85	261.75	125.76	119.58
Maltose	42.67	22.18	22.42	17.79
Isomaltose	47.53	65.22	26.47	31.24
Maltotriose	16.28	16.39	10.26	13.14
Panose	189.50	190.32	85.28	95.48
Isomaltotriose	7.67	10.46	4.19	5.98
Maltotetraose	20.58	7.84	11.97	5.14
Glucosyl-panose	30.95	33.88	15.73	15.01
Total IMO	312.53	324.14	153.76	166.01
Yield (g of IMO/g of maltose)	0.56	0.56	0.55	0.58

[a] products obtained after 24 h of reaction with enzyme concentration 1.6 U/ml , pH 4 and temperature 65°C.
[b] products obtained after 16 h of reaction with enzyme concentration 1.6 U/ml , pH 4 and temperature 65°C.

Figure 7 shows the comparison of IMO production in terms of concentration; yield productivity and residual substrate during the reaction period (60 h) at 300 g/l and 600 g/l of initial maltose. From Fig 7a, 7b it can be observed that the concentration of total IMO and productivity were higher in case of 600 g/l of initial maltose than that of 300 g/l. The IMO concentration declined beyond 16 h and 24 h in case of initial maltose concentration of 300 g/l and 600 g/l with peak values of 153.76 g/l and 312.53 g/l, respectively (Fig 7a). This indicates that a single batch reaction for 24 h at 600 g/l of initial maltose will produce 312.53 g/l of IMO in

RSCPublishing

ARTICLE

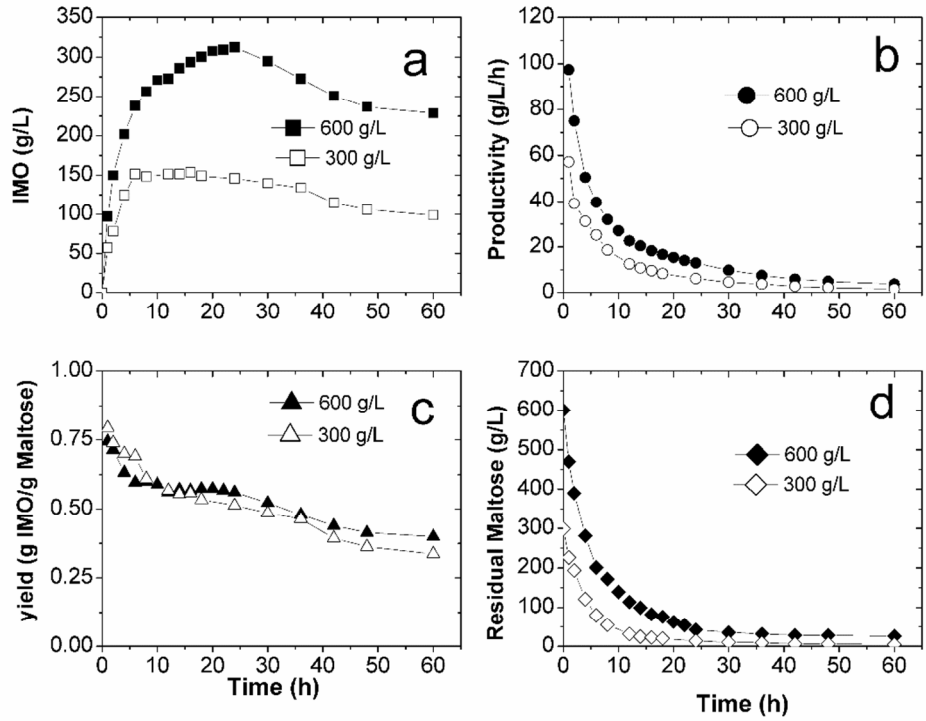

Fig 7 Comparison between (a) IMO concentration , (b) Productivity , (c) Yield and (d) Residual maltose at 600 g/l and 300 g/l (All other reaction parameters were kept same: enzyme concentration 1.6 U/ml, pH 4 and temperature 65^{o}C.)

comparison to two batch reactions for 16 h each at 300 g/l of initial maltose will produce only 307.52 g/l (153.76 x 2 g/l) of IMO.

The yield of IMO in both the cases followed similar trend without notable differences in the yield values during the time course (Fig 7c). Although yields were higher during lower time scales, it can be observed from Fig 4 and 6 that isomaltotriose production began only after 6 h and 12 h in case of initial maltose concentrations of 300 g/l and 600 g/l, respectively. This shows higher yields of IMO would not directly reflect the presence of all components contributing to net IMO. From Fig 7d it can be observed that the 92.5 % of maltose got consumed in 16 h of reaction time when 300 g/l of initial maltose was used, whereas, only 87.5 % of the maltose was consumed in case of 600 g/l for the reaction time of 24 h. The residual maltose at the end of 60 h was 4.67 g/l and 26.21 g/l for initial maltose concentration of 300 g/l and 600 g/l, respectively. Fig 7d also indicates that however long reaction time is increased there will not be complete conversion of maltose for higher dosages. From this comparison between dosage concentrations it can be concluded that higher IMO concentrations and productivities can be achieved using higher initial maltose dosage (600 g/l) for batch reactions thereby reducing the overall costs.

4. Conclusion

IMO yields were around 50% from both 60% and 30% of maltose after 24 h and 16 h reaction times, respectively. The kinetic studies revealed that there is substrate inhibition for high maltose concentration (higher than 20%) and glucose competitive inhibition. A fourteen step comprehensive model was formulated based on assumptions and experimental results. To the best of our knowledge this is the first model that takes into account the hydrolysis of IMO, substrate and product inhibition, accounting for robustness in

prediction. Parameter sensitivity analysis was carried to obtain critical parameters in the formulated model. The results predicted by the model were in agreement with the experimental data. Hence the proposed model can be used as a tool for optimization, design and control of IMO production in bioreactor.

5. Acknowledgement

Anindya Basu is thankful to Council of Scientific and Industrial Research (CSIR), India for the award of Senior Research Fellowship. The Director, CSIR- Central Food Technological Research Institute, Mysore, India is also acknowledged for supporting the work.

6. Notes

[a] Fermentation Technology & Bioengineering Department
CSIR-Central Food technological Research Institute
Email: anindya.rintu@gmail.com

[b]AcSIR – Academy of Scientific & Innovative Research
New Delhi, India

[c] Fermentation Technology & Bioengineering Department
CSIR-Central Food technological Research Institute
Email: sarma.mutturi@gmail.com

[d] Corresponding Author
Fermentation Technology & Bioengineering Department
CSIR-Central Food technological Research Institute
Telephone: 0821-2515792
Fax: 0821-2517233
Email: prapullasg@yahoo.co.in

7. Appendix:

G	Glucose
G_2^a	Maltose
G_2^b	Isomaltose
G_3^a	Panose
G_3^b	Maltotriose
G_3^c	Isomaltotriose
G_4^a	Maltotetraose
G_4^b	Glucosyl-panose
$\mathbf{v}$	Maximum velocity (g/(l.h))
$\mathbf{K_M}$	Michaelis-Menten constant (g/l)
$\mathbf{K_i}$	Inhibition constant (g/l)
$\mathbf{r}$	Rate of reaction (1,2,3,… subscripts denote equation 1, 2,3,…
$\mathbf{v_{1r}}$	Maximum velocity of hydrolysis of maltose to glucose (g/(l.h))
$\mathbf{K_{1M}}$	Michaelis-Menten constant of hydrolysis of maltose to glucose (g/l)
$K_{1iG_2^a}$	Substrate inhibition constant of hydrolysis of maltose to glucose (g/l)
$\mathbf{v_{2r}}$	Maximum velocity of hydrolysis of panose to isomaltose (g/(l.h))
$\mathbf{K_{2M}}$	Michaelis-Menten constant of hydrolysis of panose to isomaltose (g/l)
$\mathbf{v_{3r}}$	Maximum velocity of hydrolysis of panose to maltose (g/(l.h))
$\mathbf{K_{3M}}$	Michaelis-Menten constant of hydrolysis of panose to maltose (g/l)
$\mathbf{K_{3iG}}$	Competitive inhibition constant by glucose on panose as substrate (g/l)
$K_{3iG_2^a}$	Competitive inhibition constant by maltose on panose as substrate (g/l)
$\mathbf{v_{4r}}$	Maximum velocity of hydrolysis of isomaltose to glucose (g/(l.h))
$\mathbf{K_{4M}}$	Michaelis-Menten constant of hydrolysis of isomaltose to glucose (g/l)
$\mathbf{K_{4iG}}$	Competitive inhibition constant by glucose on isomaltose as substrate (g/l)
$\mathbf{v_{5r}}$	Maximum velocity of hydrolysis of maltotriose to maltose (g/(l.h))
$\mathbf{K_{5M}}$	Michaelis-Menten constant of hydrolysis of maltotriose to maltose (g/l)
$\mathbf{K_{5iG}}$	Competitive inhibition constant by glucose on maltotriose as substrate (g/l)
$K_{5iG_2^a}$	Competitive inhibition constant bymaltose on maltotriose as substrate (g/l)
$\mathbf{v_{6r}}$	Maximum velocity of hydrolysis of maltotetraose to maltotriose (g/(l.h))
$\mathbf{K_{6M}}$	Michaelis-Menten constant of hydrolysis of maltotetraose to maltotriose (g/l)
$\mathbf{K_{6iG}}$	Competitive inhibition constant by glucose on maltotetraose as substrate (g/l)
$\mathbf{v_{7r}}$	maximum velocity of hydrolysis of glucosyl-panose to panose (g/(l.h))
$\mathbf{K_{7M}}$	Michaelis-Menten constant of hydrolysis of glucosyl-panose to panose (g/l)
$\mathbf{K_{7iG}}$	Competitive inhibition constant by glucose on glucosyl-panose as substrate (g/l)
$\mathbf{v_{8r}}$	maximum velocity of hydrolysis of isomaltotriose to isomaltose (g/(l.h))
$\mathbf{K_{8M}}$	Michaelis-Menten constant of hydrolysis of isomaltotriose to isomaltose (g/l)
$\mathbf{v_{9r}}$	Maximum velocity of transglucosylation of maltose to maltotriose (g/(l.h))
$\mathbf{K_{9M}}$	Michaelis-Menten constant of transglucosylation of maltose to maltotriose (g/l)
$K_{9iG_2^a}$	Substrate inhibition constant of transglucosylation of maltose to maltotriose (g/l)

v_{10r}	Maximum velocity of transglucosylation of maltose to panose (g/(l.h))
K_{10M}	Michaelis-Menten constant of transglucosylation of maltose to panose (g/l)
$K_{10iG_2^a}$	Substrate inhibition constant of transglucosylation of maltose to panose (g/l)
v_{11r}	Maximum velocity of transglucosylation of isomaltose to isomaltotriose (g/(l.h))
K_{11M}	Michaelis-Menten constant of transglucosylation of isomaltose to isomaltotriose (g/l)
K_{11iG}	Substrate inhibition constant of transglucosylation of isomaltose to isomaltotriose (g/l)
v_{12r}	Maximum velocity of transglucosylation of maltotriose to maltotetraose (g/(l.h))
K_{12M}	Michaelis-Menten constant of transglucosylation of maltotriose to maltotetraose (g/l)
$K_{12iG_2^a}$	Substrate inhibition constant of transglucosylation of maltotriose to maltotetraose (g/l)
v_{13r}	Maximum velocity of transglucosylation of panose to glucosyl-panose (g/(l.h))
K_{13M}	Michaelis-Menten constant of transglucosylation of panose to glucosyl-panose (g/l)
$K_{13iG_2^a}$	Competitive inhibition constant by maltose on panose as substrate (g/l)
v_{14r}	Maximum velocity of transglucosylation of glucose to isomaltose (g/(l.h))
K_{14M}	Michaelis-Menten constant of transglucosylation of glucose to isomaltose (g/l)

8. References:

1. G.R. Gibson and M.B. Roberfroid, *J. Nutr.,* 1995, 125, 1401– 1412.
2. Grand View Research, Inc, http://www.grandviewresearch.com/press-elease/global-prebiotics-market.(Accessed on 30 December 2014)
3. E.B. Gore, C.H. Miller and D.F. Spandan, *J. Dent. Res*., 1988, 67, 75-81.
4. D. C. Sheu, C. I. Huang and K. J. Duan, *Biotechnol. Tech*., 1997, 11, 5, 287-291.
5. S.H. Yoo, M.R. Kweon, M.J. Kim, J.H. Auh, D.S. Jung, J.R. Kim, C Yook, J.W. Kim and K.H. Park, *J. Food. Sci*., 1995, 60, 516-519.
6. J.W. Yun, M.G. Lee and S.K. Song, *Biotechnol. lett*., 1994, 16, 1145-1150.
7. Y.M. Park and I.S. Chung, *Biotechnol. Tech*., 1998, 12, 19989, 667-669.
8. F. L. Arrojo, D. Marin, A.G. Segura, D. Linde, M. Alcalde, P.G. Alonsob, I. Ghazia , F.J. Ploua, M.F. Lobato, and A. Ballesterosa, *Process Biochem*., 2007, 42, 1530-1536.
9. K.J. Duan, D.C. Sheu and C.T. Lin, *Ann. N. Y. Acad. Sci*., 1995, 750, 325–328.
10. K.J. Duan, D.C. Sheu, M.T. Lin and H.C. Hsueh, *Biotechnol. lett*., 1994, 16, 11, 1151–1156.
11. K. Deb, in Optimization for Engineering Design: Algorithms and Examples, 2004, PHI Learning Pvt. Ltd., Ch. 6, 290-356.
12. R. Moros, H. Kalies, H.G. Rex and S. Schaffarczyk, *Comp. Chem. Eng*., 1995 20, 1257.
13. G.F. Froment and T.Y. Park, *Comp. Chem. Eng*., 1998, 22, 103-110.
14. C.Y. Gau, J.F. Brennecke and M.A. Stadtherr, *Fluid Phase Equilib*., 2000, 168, 1-18.
15. D.C. Khandekar, T. Palai, A. Aragwal and P.K. Bhattacharya, *Bioprocess Biosyst. Eng,* 2014, DOI 10.1007/s00449-014-1230-5.
16. A. Basu and S.G. Prapulla, Unpublished work.
17. N. Kato, S. Suyama, M. Shirokane, M. Kato, T. Kobayashi and N. Tsukagoshi, *Appl. Environ. Microb*., 2002, 68, 1250-1256.
18. K.H. Jung, J.W. Yun, K.R. Kang, J.Y. Lim and J.H. Lee, *Enzyme Microb. Technol*., 1989, 11, 491-494.
19. F.M. Rodriguez, C.A. Cardelle, M. Villamiel and J.R. Banga *J. Biotechnol.,* 2011, 3-4, 116-124.
20. D.E. Goldberg in Genetic Algorithms, Addison Wesley, New York. , 1989.
21. R. Ashino, M. Nagase and R Vaillancourt, *Comput Math Appl*., 2000, 40, 491-512.
22. M.B. Alvarado-Huallanco, and F. Maugeri-Filho J. *Chem. Technol. Biotechnol.,* 2010, 85, 12, 1654–1662.
23. Y. Konishi and K. Shindo, *Biosci. Biotech. Bioch*., 1997, 61, 439-442.
24. I. Kobayashi, M. Tokuda, H. Hashimoto, T. Konda, H. Nakano and S. Kitahata, *Biosci. Biotech. Bioch.,* 2003, 67, 29-35.
25. C. Pertev, M. Turker and R. Berber, *Comp. chem. Eng,* 1997, 21, S739-S744.

Fig 1

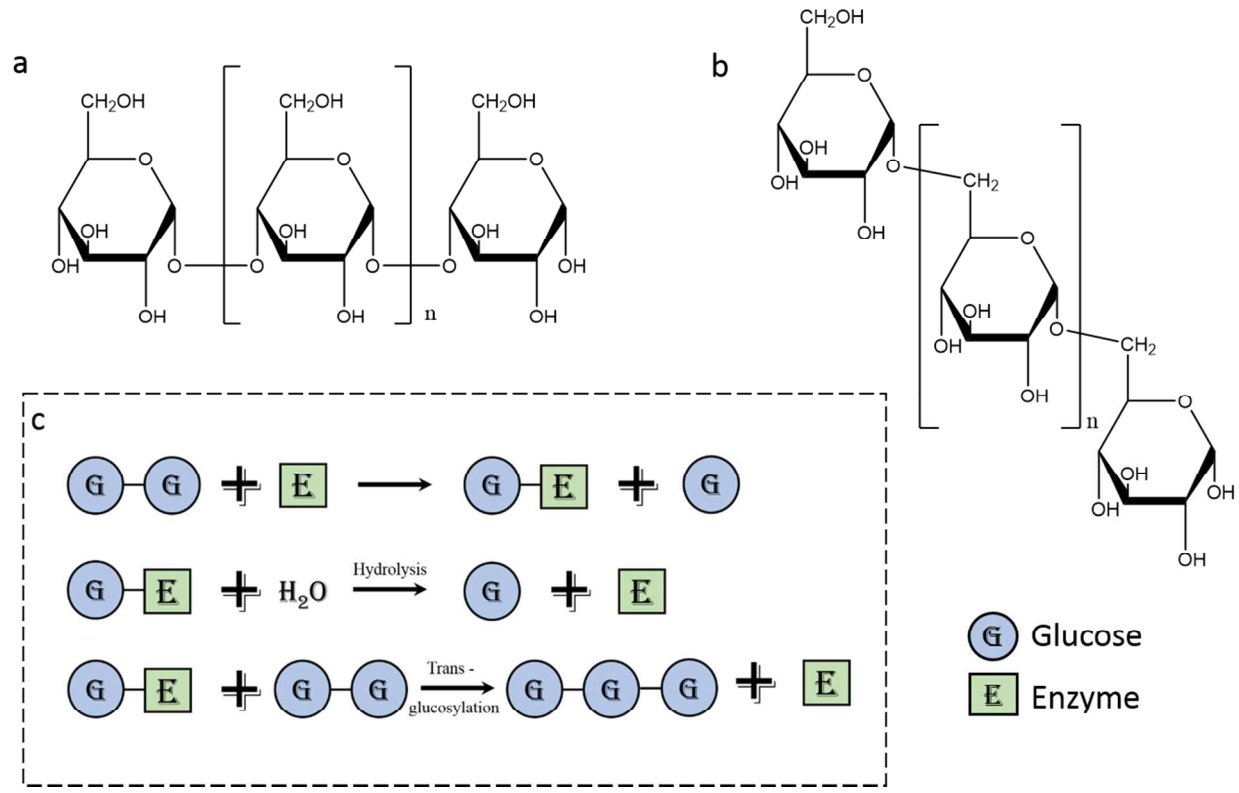

Fig 2

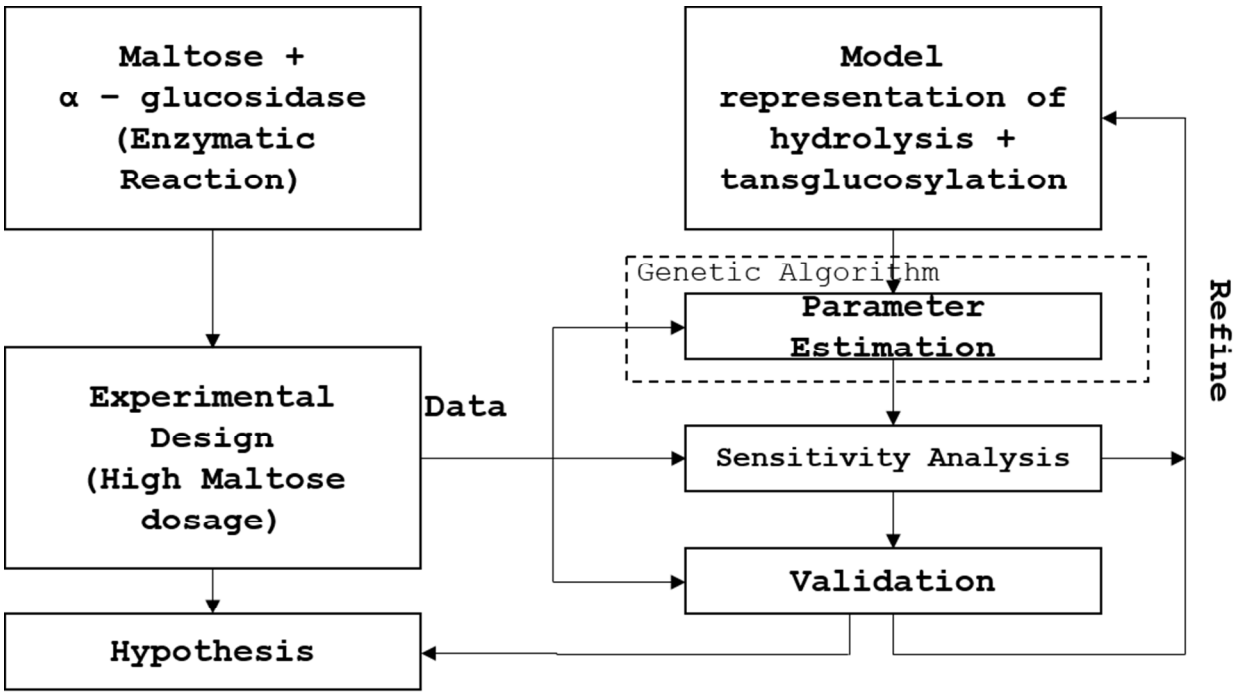

Fig 3

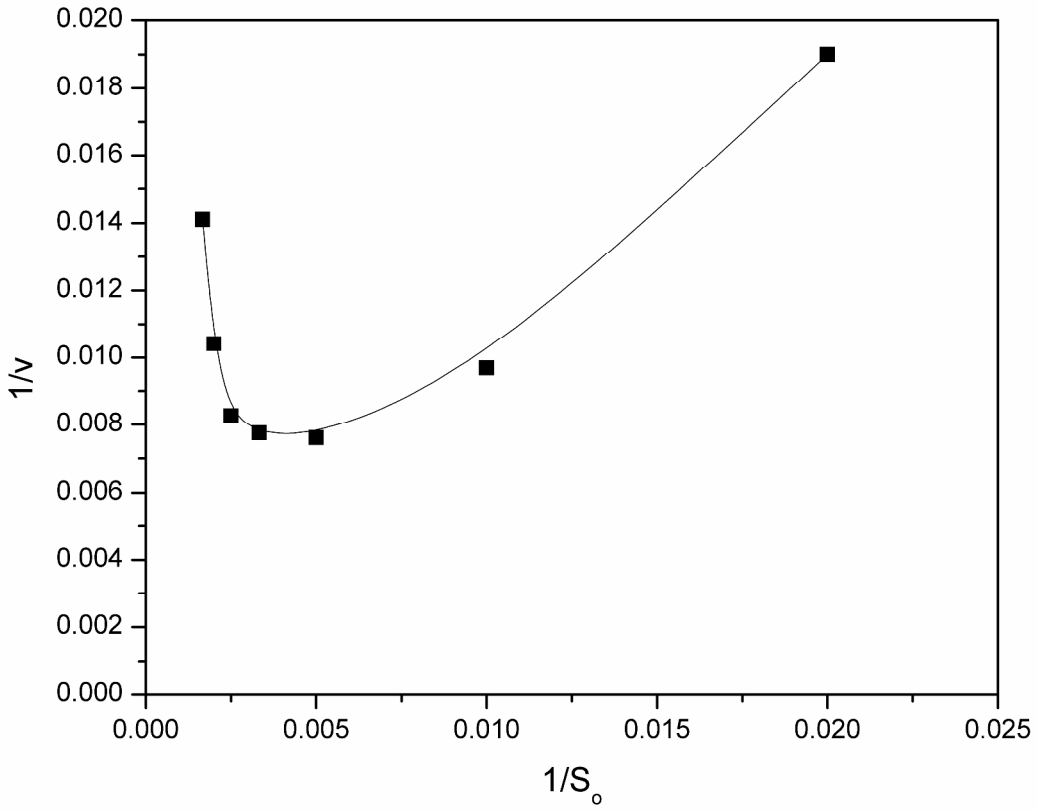

Fig 4

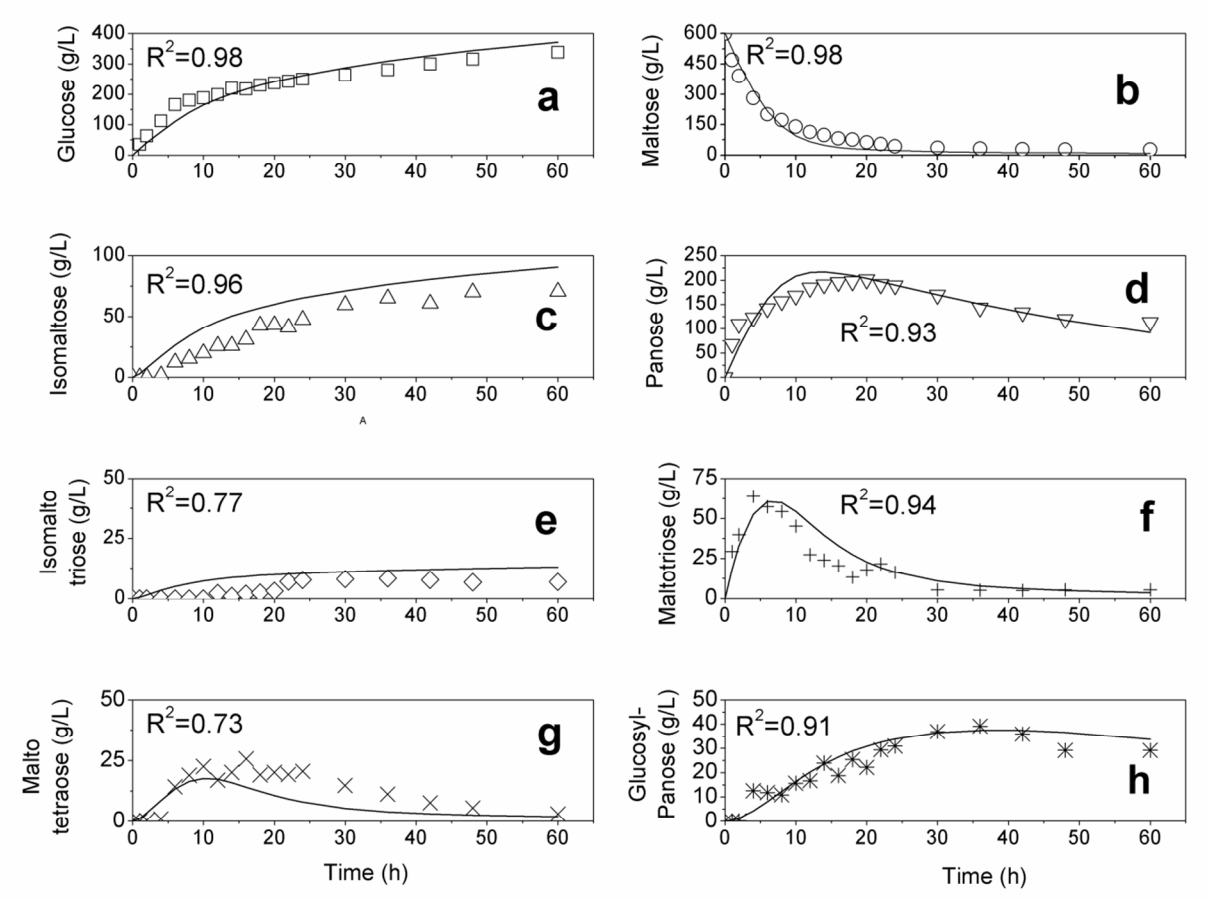

Fig 5

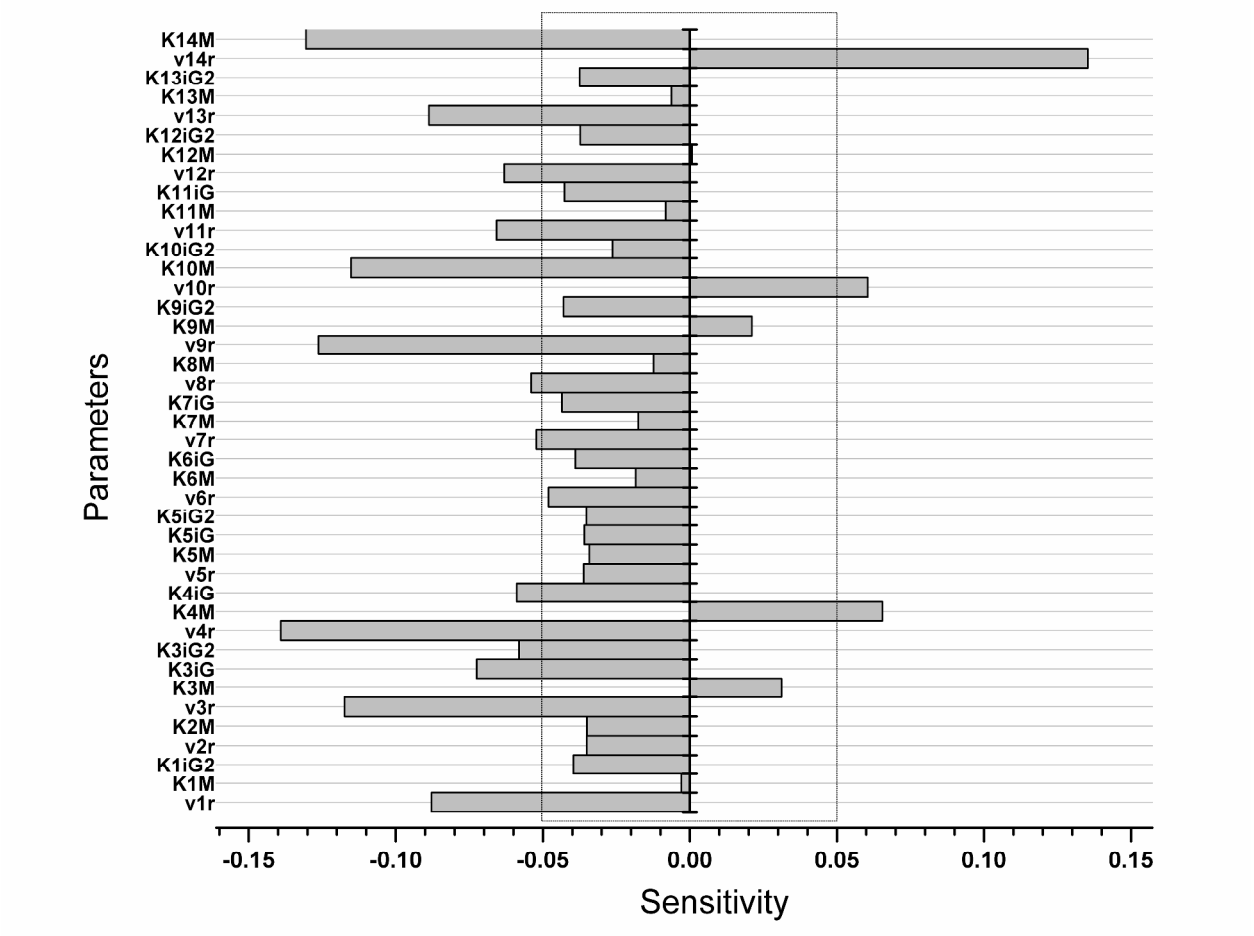

Fig 6

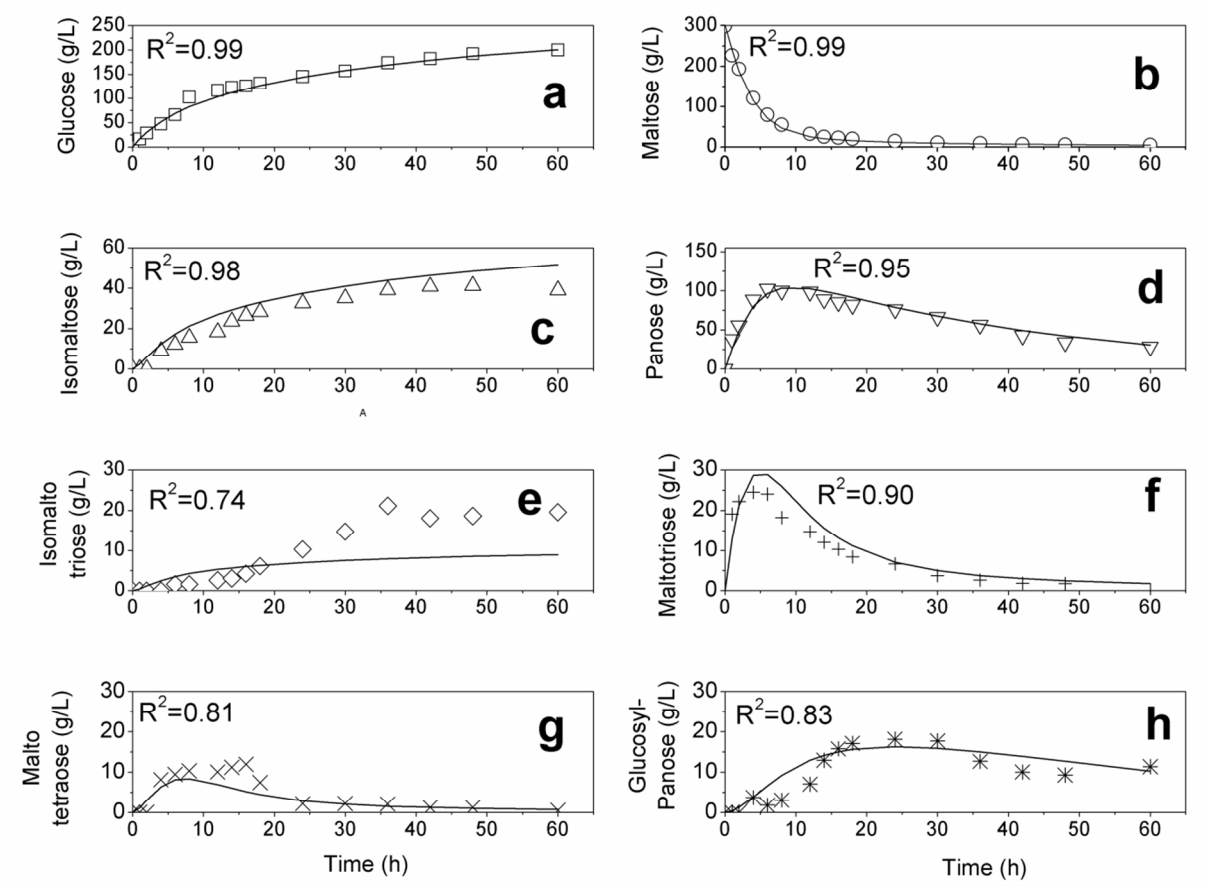

Fig 7